Desalination and Water Treatment
www.deswater.com
47 (2012) 300–309
September

doi: 10.1080/19443994.2012.696419
Taylor & Francis
Taylor & Francis Group

Comparative study on the adsorption of malathion pesticide by different adsorbents from aqueous solution

Ahmed M. Donia[a,*], Asem A. Atia[a], Rashad A. Hussien[b], Rama T. Rashad[b]

[a]*Faculty of Science, Department of Chemistry, Menoufia University, Egypt*
Tel. +20 17 6130046; Fax: +20 38356313; email: ahmeddonia2003@yahoo.com
[b]*Soil, Water and Environment Research Institute, Agricultural Research Center, Giza, Egypt*

Received 3 September 2011; Accepted 12 March 2012

ABSTRACT

A study on the adsorption behavior and removal of an organophosphorous pesticide, malathion, from aqueous solution was carried out using batch method. The activated charcoal and bentonite clay were selected as commonly used adsorbents to be compared to a less commonly used kaolinite clay. Two thermally treated kaolinite samples were prepared at different temperatures. The samples were investigated by means of X-ray powder diffraction and thermogravimetric analysis. In aqueous medium, the thermally treated clay samples displayed higher adsorption capacities ($q_e = 356.06$ and $362.37\ \mu mol\ g^{-1}$, for kaolinite, and $282.32\ \mu mol\ g^{-1}$, for bentonite) relative to that of the untreated one ($q_e = 311.87\ \mu mol\ g^{-1}$, for kaolinite, and $188.13\ \mu mol\ g^{-1}$, for bentonite). In addition, the thermally treated kaolinite samples exhibited faster adsorption rates ($k_1 = 3.03 \times 10^{-3}$ and $2.77 \times 10^{-3}\ min^{-1}$) compared with that of the untreated one ($k_1 = 1.84 \times 10^{-3}\ min^{-1}$). Desorption of malathion from the loaded samples was also carried out for regeneration purposes. The adsorption/desorption cycle of malathion on the kaolinite samples was repeated several times and the removal efficiency of the regenerated kaolinite sample was noticed to decrease after the 3rd cycle.

Keywords: Malathion; Adsorption: Kaolinite; Bentonite; Insecticides; Isotherms

1. Introduction

Water pollution by organic and inorganic compounds is of great public concern. Pesticides are very dangerous and harmful because of their toxic and carcinogenic nature. They contaminate water through agricultural, domestic and industrial activities and therefore, their removal is important [1,2]. They are mostly dissolved in water and cannot be easily removed by solid/liquid separation process such as coagulation and sand filtration. An effective and simple method is the addition of powdered activated carbon (PAC) at the inlet of a water purification process train [3]. Due to the higher cost of activated carbon, attempts had been made to find out alternative adsorbents for pesticides removal such as bentonite clays, kaolin, iron oxides, and so on [4–7]. Organoclays have been considered as good adsorbents of nonionic organic contaminants. The hydrophilic surface of clay changes into hydrophobic that sorbs effectively organic compounds from water and air, through formation of particular types of aggregates during coagulation. The aim is to reduce the amounts of pesticides distributed in the environment [8–10].

Clay minerals provide different adsorption sites for neutral molecules (external and internal cations, surface oxygen atoms, silanol and aluminol groups at

*Corresponding author.

the edges, etc.). A further possibility is opening the interlayer spaces by pillaring reactions to promote penetration of pesticides molecules among layers. The adsorption properties of bentonites are changed when they are calcined at 350–550°C, i.e. at conditions that layer structure is retained. These changes can be used to enhance pesticide adsorption as previously stated for metolachlor [11]. Calcination (thermal treatment at different temperatures) of clay minerals leads to dehydration and dehydroxylation processes and can be accompanied by movements of the octahedral cations within the octahedral sheet. This leads to improved hydrophobicity without need to prepare organoclay through cation exchange with organic cations [12,13].

The present work is a comparative study on the capacity and/or efficiency of calcined kaolinite and bentonite minerals compared to the commonly used activated charcoal (AC) in the removal of a partially hydrophobic organophosphorous pesticide (as a simple model: malathion) from aqueous solution. The main goal is to assess the role of difference in the hydrophilic–hydrophobic nature of the clay surface; sometimes related to thermal treatment; in directing the interaction between the adsorbate and the adsorbent. The study was carried out under different conditions such as dose of adsorbent, concentration of pesticide, time of contact, the type of medium, and temperature.

2. Materials and methods

2.1. Materials

2.1.1. Malathion

An organophosphorous pesticide was selected. The pesticide was s-1,2-bis (ethoxy carbonyl) ethyl *o,o*-dimethyl phosphorodithioate (malathion) (Fig. 1). Its molecular formula $C_{10}H_{19}O_6PS_2$ and formula weight is 330 g/mol. Water solubility = 145 mg/L [5,8].

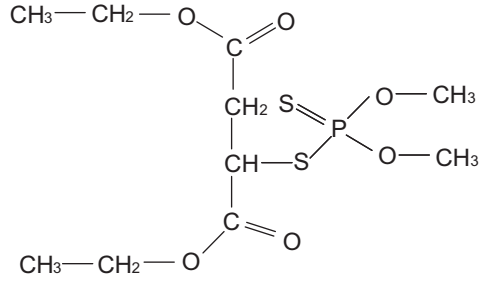

Fig. 1. Malathion: s-1,2-bis (ethoxy carbonyl) ethy *o,o*-dimethyl phosphorodithioate.

2.1.2. Adsorbents

AC was supplied by Adwic Co., General Purposes Reagents G.P.R. Egypt. Bentonite was Sigma-Aldrich (cation exchange capacity CEC = 44.2 cmol kg^{-1} [14]), and kaolinite was Merck product, Aluminum Silicate Hydroxide ($\sim Al_2Si_2O_5(OH)_4$), CEC = 12.9 cmol kg^{-1}). The natural bentonite sample (B1) was thermally treated for 2 h in a muffle furnace at 550°C to obtain B2. Similarly, the natural kaolinite (K1) was thermally treated at 400 and 600°C to obtain K2 and K3, respectively [14,15].

2.2. Methods

2.2.1. Malathion solution

A 100 μg mL^{-1} stock solution of malathion in distilled water was prepared. It was scanned at different wavelengths (175–400 nm) using JENWAY 6405 UV/Vis, UK. Spectrophotometer. Different concentrations of malathion in distilled water were obtained by dilution of the 100 μg mL^{-1} stock. The absorbance of these concentrations was measured at $\lambda = 195$ nm and the calibration curves were drawn [5,8].

Calibration curves at $\lambda = 200$ nm of malathion in methanol (MeOH), 50% MeOH/aqueous mixture and 0.001 M NaCl solution were prepared using the same previous procedure Fig. 2.

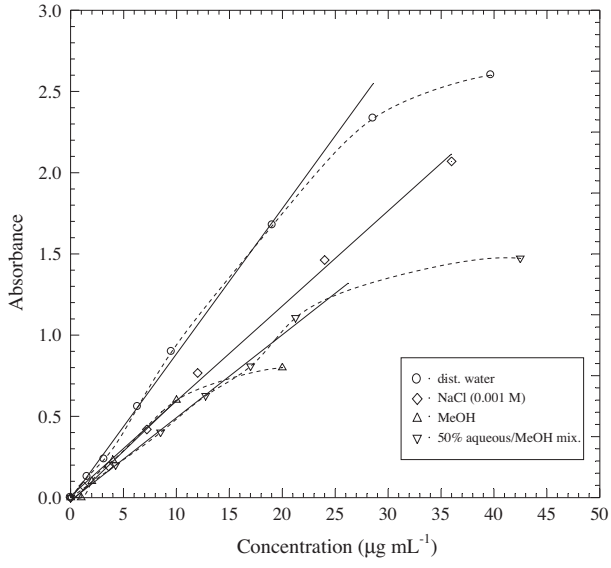

Fig. 2. Calibration curves of malathion in distilled water, NaCl (0.001 M), MeOH, and 50% aqueous/MeOH mixture at natural pH.

2.2.2. Adsorption studies

Effect of adsorbent dose. Different portions (0.03–0.15 g) of each adsorbent were placed in a series of flasks containing 50 mL aqueous solution of malathion with initial concentration 100 μg mL^{-1} at natural pH (6.0). The flasks were shaken on Vibromatic–384 at 300 rpm at 18˚C for 1 h and left overnight for equilibrium. The absorbance of residual concentration of malathion was measured and the amount adsorbed by each adsorbent samples (q_e, μmol g^{-1}) was calculated according to Eq. (1) [16]:

$$q_e = \frac{(C_0 - C)}{m} \times \frac{V}{330} \quad (1)$$

where C_0 and C are the initial and final concentration of malathion (μg mL^{-1}), respectively, V is the volume of solution (L), m is the weight of adsorbent (g), and 330 is the molecular weight of malathion (g mol^{-1}).

Effect of contact time. Portions of 0.03 g of studied adsorbents were placed in a series of flasks. To each flask, 50 mL aqueous solution (100 μg mL^{-1}) of malathion at natural pH (6.0) was added and were shaken on Vibromatic–384 at 300 rpm at 18˚C. Five milliliters of the solution were taken at different time intervals (from 2.5 min to 24 h). The absorbance of residual concentration of malathion was measured and the amount adsorbed by each adsorbent samples (q_e, μmol g^{-1}) was calculated according to Eq. (1).

Effect of initial concentration of malathion. Portions of 0.03 g samples of all adsorbents were placed in a series of flasks containing 50 mL of malathion solution with different concentrations at natural pH (~6.0). The contents of the flasks were shaken at 300 rpm and 18˚C for 6 h for AC, B1, B2, and for overnight for K1–K3 samples. After equilibration, 5 mL of the solution were taken for the determination of residual concentration of malathion using UV-spectrophotometer. The amount adsorbed then calculated.

Effect of temperature. Portions of 0.03 g samples of K1 and K3 were placed in a series of flasks containing 50 mL of malathion solution with different concentrations at natural pH (~6.0). The contents of the flasks were shaken in a water bath at 300 rpm and at 18˚C, 50˚C, and 60˚C for overnight. After equilibration, 5 mL of the solution were taken for the determination of residual concentration of malathion using UV-spectrophotometer. The amount adsorbed then calculated.

2.2.3. Desorption studies

Two grams of each adsorbent were loaded by malathion through shaking for 1 h then soaking in malathion solution (100 μg mL^{-1}) overnight. The loaded adsorbents were filtered off, washed by distilled water and then dried at 40˚C for 2 h. The uptake value was calculated. The loaded samples of AC, B2, and K3 were heated (in the atmospheric air) in a muffle furnace at different temperatures (150, 250, 350, 500, and 650˚C) for 2 h. The uptake of malathion from aqueous solution by heated samples (after desorption of malathion) was calculated for the second run. The higher desorption percentage was obtained for the regenerated sample at 500˚C. The sorption/desorption cycles were repeated at 500˚C for four runs.

2.3. Instrumentation

Thermogravimetric analysis (TGA) and differential thermal analysis (DTA) were applied in order to observe the reactions taking place during the thermal treatment of the K1 and malathion-loaded K3 samples using Shimadzu DTA/TGA-50, Japan.

An X-ray diffractometer (XRD), SCINTAG/USA, with Ni-filtered Cu K_α radiation, was used for determining the mineral contents of the K1–K3 samples and the phase formation during calcination.

Fourier transform infrared (FT-IR) measurements were used to characterize malathion, K1, K3, and malathion-loaded K3 using FT-IR Nexeus-Nicolette Model 640-MSA. The dried samples were ground with KBr and then compressed as pellets under hydraulic pressure. The pellets obtained were oven dried again at 70˚C for 1 h and used for FT-IR measurements.

3. Results and discussion

3.1. Adsorption studies

3.1.1. Effect of adsorbent dose

Adsorption of malathion on the studied adsorbents as a function of adsorbent dose was shown in Fig. 3(a) and (b). The adsorption capacity of malathion (μmol g^{-1}) from aqueous solution decreases as the solid/liquid (S/L) ratio increases (Fig. 3(a) and (b). The highest value in the studied range was obtained at 0.03 g/50 mL S/L ratio, while the lowest one was at 0.15 g/50 mL S/L ratio. As the solid weight increases in solution, the suspended particles increase and may coagulate and/or agglomerate. So, the available surface area exposed to adsorbate decreases despite of increasing weight and hence the adsorption capacity of adsorbate decreases [17].

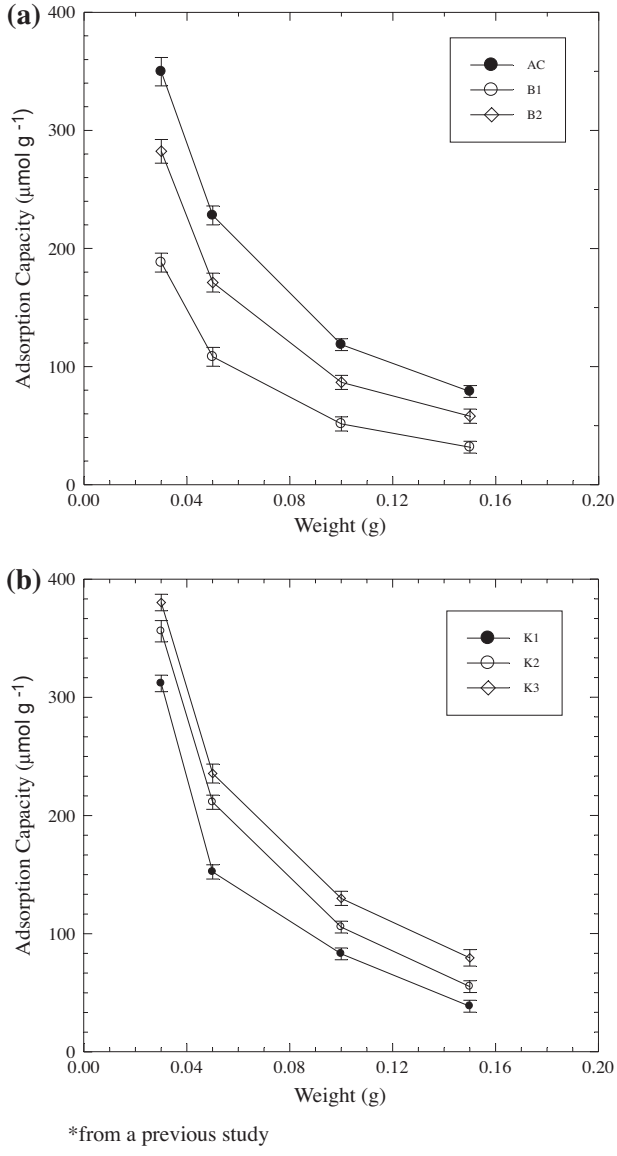

Fig. 3. Effect of adsorbent dose on the adsorption of malathion from aqueous solutions at $C_i = 100\,\mu g\,mL^{-1}$, equilibrium time 24 h, pH 6, and at 18°C (error bars represent the standard deviation of three replicates). (a) By AC, B1, and B2, (b) by K1, K2, and K3 * from a previous study [17].

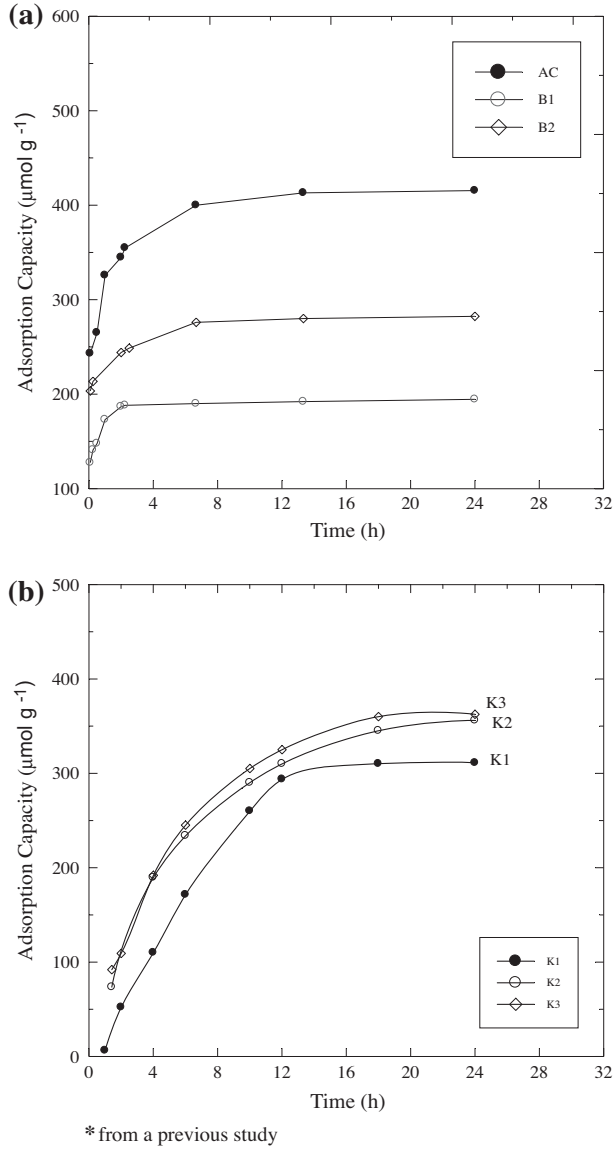

Fig. 4. Effect of contact time on the adsorption of malathion from aqueous solutions at $C_i = 100\,\mu g\,mL^{-1}$, pH 6, and at 18°C. (a) By AC, B1, and B2, (b) by K1, K2, and K3 * from a previous study [17].

3.1.2. Effect of time

The removal of malathion in aqueous solution by different adsorbents increases with increasing time of contact till reach equilibrium after 6 h for AC, B1 and B2, and overnight for K1–K3 samples. Fig. 4(a) and (b) indicates that the calcined clay samples, K2, K3, and B2 have higher adsorption capacity (comparable with AC) than that of the noncalcined K1 and B1.

3.1.3. Effect of concentration

Adsorption isotherms of malathion in aqueous solution on the studied adsorbents are shown in Fig. 5(a) and (b). The adsorption capacity values (μmol g^{-1}) of malathion increased in the order B1 < B2 < K1 < K2 < K3 < AC. For B1, K1, K2 and K3, as the malathion concentration increases in solution, its adsorption capacity increases steadily and before the plateau completion a second increase in the adsorption capacity value occurs.

It was previously established that calcination of clay minerals improves their surface hydrophobicity

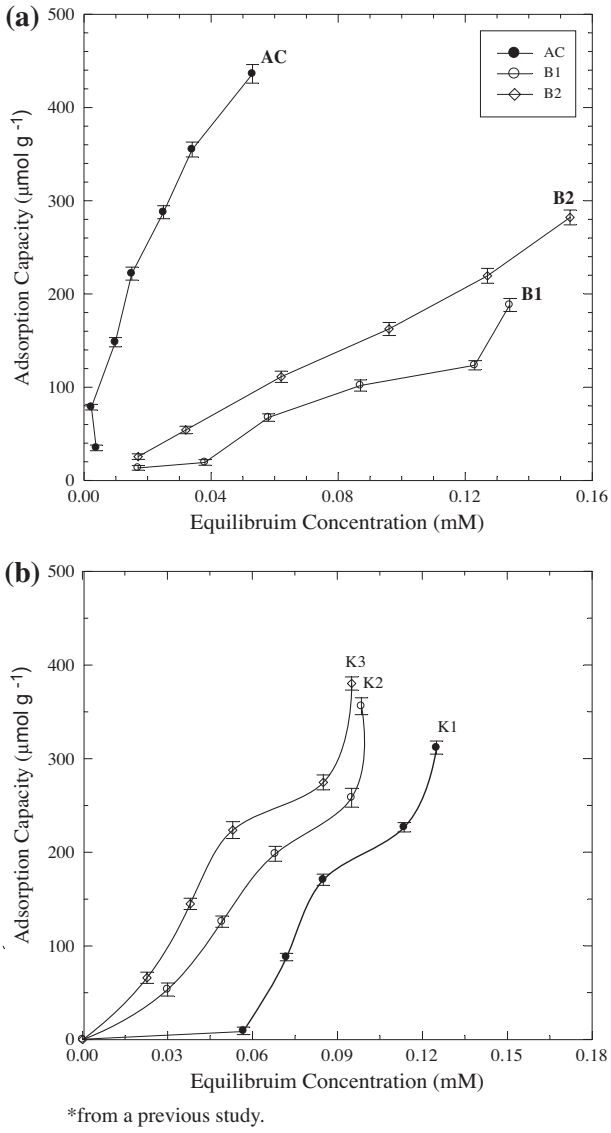

Fig. 5. Adsorption isotherms of malathion in aqueous solutions at pH 6 and at 18˚C (error bars represent the standard deviation of three replicates). (a) By AC, B1, and B2, (b) by K1, K2, and K3 * from a previous study [17].

(CEC values of kaolinite samples decreased by thermal treatment, 7.13 and 4.88 cmol kg^{-1} for K2 and K3, respectively) [18,19]. So, better hydrophobic interaction expected to occur among the partially hydrophobic malathion molecules, as being sparingly soluble in water, and calcined clay surfaces. At low concentration, adsorbate molecules may interact individually with the clay particles surface. At higher concentration, adsorbate–adsorbate interactions at the surface may occur, due to crowded hydrophobic molecules, forming a second layer of adsorbate. The aqueous medium improved this behavior, i.e. thermal treatment of clay improved the removal of malathion from aqueous solution.

Same trend was observed in the electrolytic aqueous medium (0.001 M NaCl solution) and aqueous–organic mixed medium (50% aqueous/MeOH solution) Fig. 6(a) and (b). In a pure organic medium (MeOH), no adsorbate–adsorbate interaction occurred at higher concentration [17]. Good solvation (separation) of the hydrophobic adsorbate molecules prevents the formation of second layer of adsorbate. Also, no observed difference in adsorption capacity values between calcined K3 and noncalcined K1 samples and maximum adsorption capacity corresponds to the

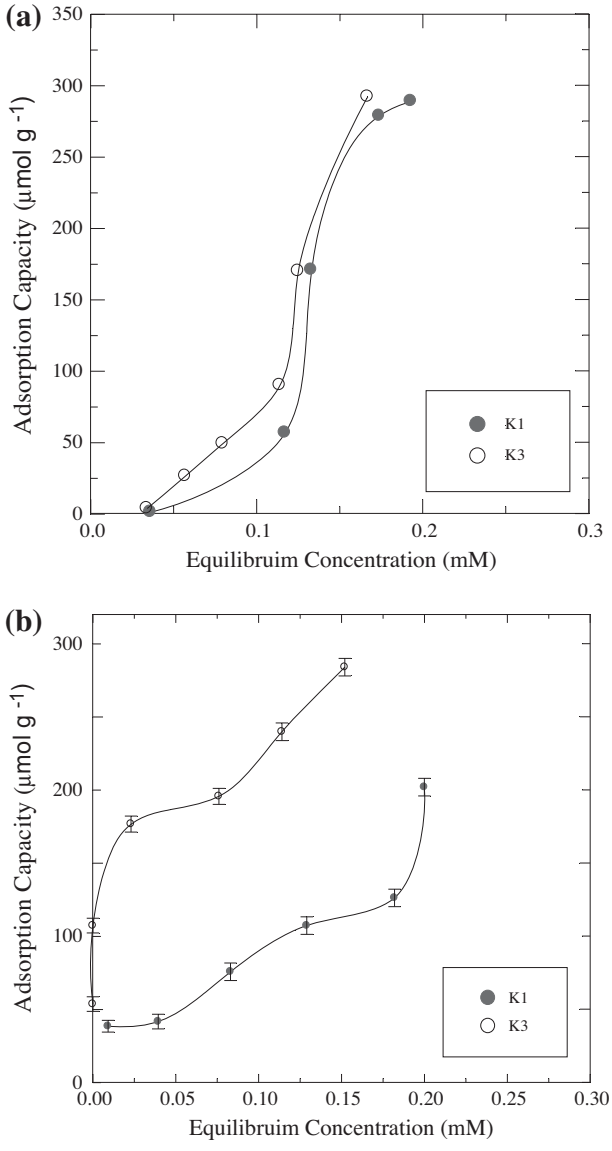

Fig. 6. Adsorption isotherms of malathion on K1 and K3 at natural pH 6 and 18˚C: (a) in 50% aqueous/MeOH solution, (b) in 0.001 M NaCl solution.

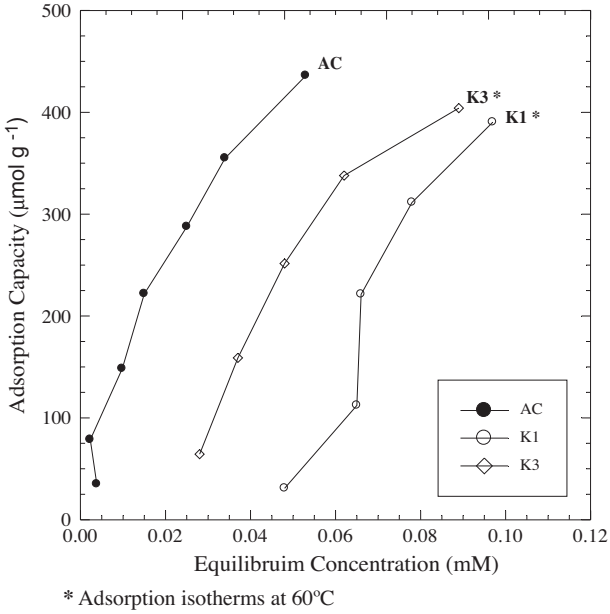

Fig. 7. Adsorption isotherms of malathion in aqueous solution at natural pH by AC (at 18℃), K1, and K3 at 60℃.

monolayer adsorption (141.3 μmol g^{-1}) [17]. The hydrophobicity improved by calcination disappeared in the pure organic medium.

Fig. 7 is a comparison between the adsorption isotherms of malathion in aqueous solution for AC at 18℃, and for K1, and K3 at 60℃. According to Giles classification system, the shape of the isotherm can be used to classify the adsorption mechanism [20]. It was observed from Fig. 7 that; at 60℃, the monolayer portion of the isotherms disappears and the multilayer portion is predominant, which is almost the same trend observed for the adsorption of malathion by AC. A difference still exists between the calcined K3 and the noncalcined K1 samples. The continuous increase in the adsorption capacity may indicate an endothermic process which involves one or more mechanism:

(i) Multilayer adsorption of malathion species on the clay surface, and/or
(ii) Coagulation of the clay particles carrying the adsorbate molecules forming aggregates [20–23].

3.2. Modeling of malathion adsorption by kaolinite

3.2.1. Kinetics

The adsorption data of malathion by AC, B1, B2, K1, K2, and K3 in Fig. 4 were treated according to the pseudo-first and pseudo-second-order kinetics, Eqs. (2) and (3), respectively [24]:

$$\log[q_t - q_e] = \log q_{max} - \frac{k_{ads}\, t}{2.303} \quad (2)$$

where q_e and q_t refer to the adsorption capacity of malathion (μmol g^{-1}) at equilibrium and at time t (min), respectively and k_{ads} is the overall rate constant of pseudo-first-order reaction. Plotting $\log[q_t - q_e]$ vs. t (min) gives a straight line with a slope = $-(k_{ads}/2.303)$ and intercept $\log q_{max}$.

$$\frac{t}{q_t} = \left(\frac{1}{k_2 q_e^2}\right) + \left(\frac{t}{q_e}\right) \quad (3)$$

where k_2 (g $mmol^{-1}$ min^{-1}) is the overall rate constant of the pseudo-second-order kinetics.

It is obtained from the slope and intercept of the straight line of (t/q_t) vs. t (min). The kinetic parameters of the studied adsorbents are listed in Table 1.

For kaolinite samples, the rate constant values have increased in the direction of increasing the calcination temperature. The validity of pseudo-first-order model for malathion adsorption implies that one term affects the rate of reaction, either adsorbate concentration or surface properties.

Table 1
Kinetic data for the adsorption of of malathion by different adsorbents

Adsorbent	Exp. q_{max} (μmol/g)	q_e (μmol/g)	$K^{*,**}$	R^2
Charcoal**	354.8	368.8	0.0004	0.994
B1**	188.13	195.67	0.0008	0.998
B2**	282.32	281.40	0.0003	0.999
K1*	311.87	334.97	0.0018	0.949
K2*	356.06	342.17	0.0028	0.995
K3*	362.37	353.19	0.0030	0.999

*Pseudo-first-order, k_{ads} (min^{-1}).
**Pseudo-second-order, k_2 (g μmol^{-1} min^{-1}).

Table 2
Intraparticle diffusion parameters for the adsorption of malathion by different adsorbents

Adsorbent	K_{dif} (μmol g^{-1} $min^{-0.5}$)	X_i	R^2
Charcoal	11.99	215.29	0.897
B1	6.62	114.41	0.977
B2	3.44	196.80	0.784
K1	11.06	−56.32	0.913
K2	9.60	29.41	0.914
K3	10.09	25.79	0.923

The hydrophobic interaction and bilayer adsorption suggestion may refer to the formation of specific aggregated structures of adsorbate–adsorbent composites. Hence, intraparticle diffusion may occur.

The adsorption capacity time data were treated according to the intraparticle diffusion Eq. (4). [25–27]:

$$q_t = X_i + K_{dif}\, t^{0.5} \quad (4)$$

where X_i is the external film resistance (the boundary layer diffusion effects); K_{dif} is the intraparticle diffusion rate constant (μmol g^{-1} $min^{-0.5}$). When the adsorption system involves an intraparticle diffusion step, plotting q_t against $t^{0.5}$ gives a straight line with a slope and an intercept representing K_{dif} and X_i, respectively. As the value of X_i decreases the effect of external film resistance on the reaction rate decreases [25–27].

According to Table 2, the k_{dif} values for the K2 and K3 samples were lower than that of K1, i.e. the rate of diffusion was faster for K1 than for calcined samples. The effect of the external film resistance on the adsorption rate increased in the order K1 < K2 < K3 in aqueous medium as indicated by the positive values of X_i.

Therefore, the rate of malathion adsorption by calcined samples is mainly controlled by the intraparticle diffusion as a diffusion in the boundary layer. The faster rate of diffusion and the lower external film resistance for K1 may be related to its hydrated surface before calcination (hydrophilic nature). Water molecules at the surface of the clay may play an important role in the retention of malathion molecules at the hydrophobic adsorption sites (silane Si–O) on the clay surface.

One suggested mechanism is the formation of Water Bridge through H-bonding between the clay surface and the electron rich side of malathion molecule containing O, S, and P atoms. The FT-IR spectral analysis of malathion-loaded K3 may support this concept.

For bentonite clay mineral, same trend still exists. But the K_{dif} values are lower than those for kaolinite. In addition, the values of X_i are greater than those for kaolinite. The higher concentration of counter ions on B1 surface (higher CEC value than kaolinite) may increase the effect of external film resistance which, in turn, affects the rate of interaction between malathion molecules and adsorbent surface [25–27].

3.2.2. Freundlich model

Data of malathion adsorption capacity by different adsorbents (Fig. 5) were treated by Freundlich model for adsorption Eq. (5) [24]:

$$Cs = K_F C_{eq}^{n_F}$$

$$\log Cs = \log K_F + n_F \log C_{eq} \quad (5)$$

where Cs is the amount adsorbed of malathion (μmol g^{-1}), C_{eq} is the equilibrium concentration (μM), K_F [(μmol g^{-1})(L μmol^{-1})] and n_F are Freundlich parameters obtained from the intercept and slope of the straight line of log Cs vs. log C_{eq}. Their values are listed in Table 3.

The values of affinity constant, K_F, followed the order AC > K3 > B2 > K2 > B1 > K1, i.e. the affinity between adsorbate and adsorbent surface was greater for the modified clay minerals (although their slower intraparticle diffusion rate) than the nonmodified minerals. This confirms the improved hydrophobicity of the calcined surface through thermal treatment and the enhanced hydrophobic–hydrophobic interaction between malathion molecules and calcined surface sites.

The n_F values followed the order AC < B2 < K3 < B1 < K2 < K1. All values of $n_F > 1$, indicating an *S*-type isotherm (cooperative process, may be multilayer adsorption, i.e. adsorbate–adsorbate

Table 3
Freundlich parameters for the adsorption of malathion by different adsorbents

Adsorbent	K_F (μmol/g) (L/μmol)	n_F	R^2
Charcoal	10.54	1.02	0.946
B1	2.86×10^{-1}	1.30	0.938
B2	1.27	1.07	0.998
K1	3.22×10^{-6}	3.86	0.829
K2	3.88×10^{-1}	1.47	0.972
K3	2.35	1.11	0.955

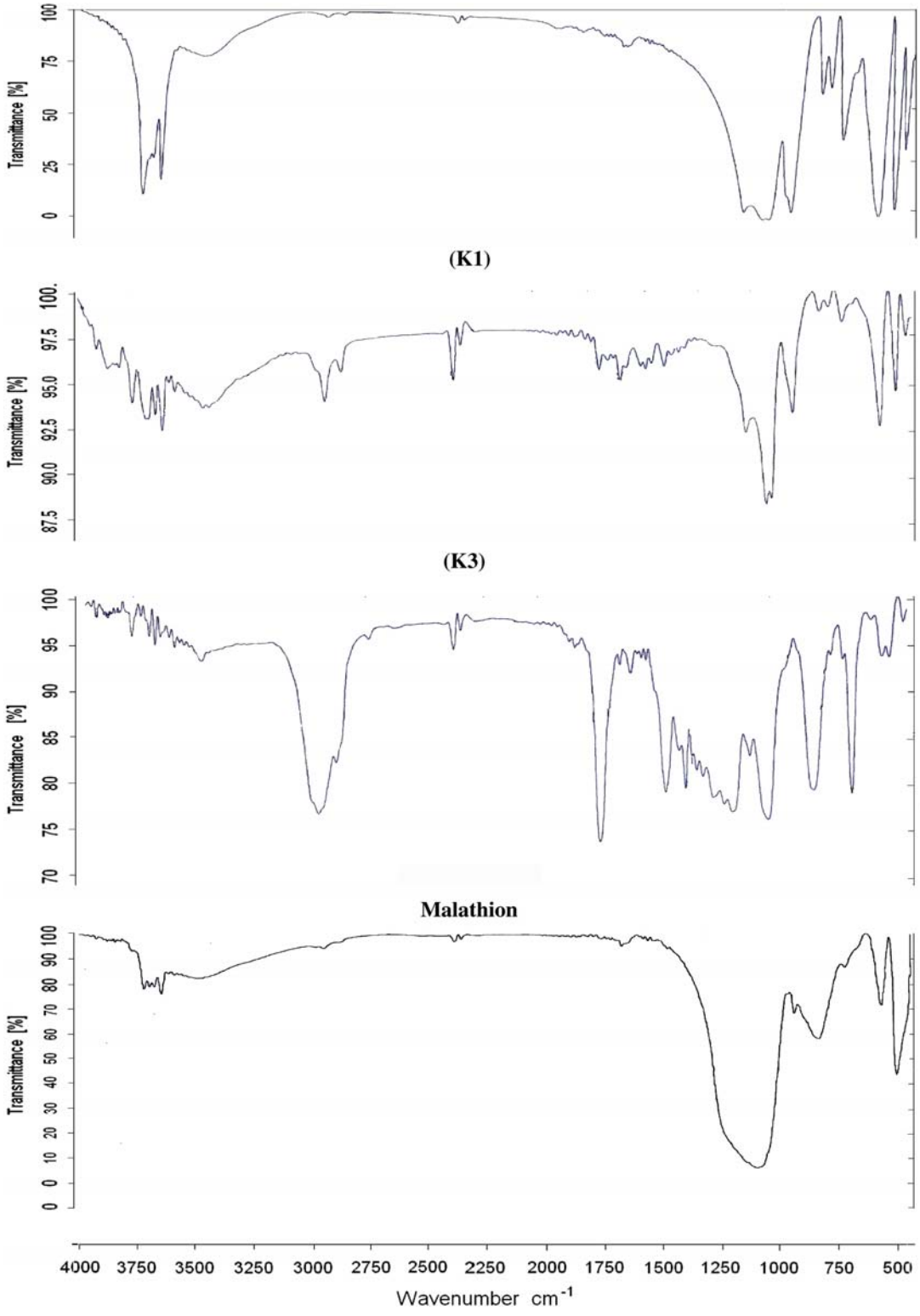

Fig. 8. FT-IR spectra for malathion, K1, K3, and malathion-loaded K3.

interaction at the surface) [22–26]. The values of the modified samples were closer to the 1 value than the nonmodified samples. The minimum value of AC (1.02) is near the *C*-type isotherm (coagulative process, may be aggregates formation, i.e. adsorbent–adsorbent particles interaction).

Table 4
Regeneration of the studied adsorbents at 500°C

Adsorbent	Exp. q_{max} (μmol/g)	2nd run of regeneration	3rd run of regeneration	4th run of regeneration
AC	436.00	466.15	432.55	189.91
B1	188.13	352.27	346.10	203.27
B2	282.32	329.83	193.87	173.61
K1	311.87	346.59	341.29	178.95
K3	362.37	396.29	364.47	213.34

4. Characterization of kaolinite

4.1. Thermal decomposition

The TGA analysis of K1 exhibits main changes during heating of the natural K1. A number of weight losses near 350 and 600°C and above 600°C. The first loss can be assigned to a low temperature release of adsorbed water on surfaces, in the pores, in the bulk of kaolinite particles, and in the channels that are attached to the sides of the silicate units. The loss of such adsorbed water is more gradual and may persist continuously to temperatures higher than 100–150°C. Weight loss due to a predehydration process first occurring at the –OH of the surface can occur up to ~400°C. It may be a result of reorganization in the octahedral layer, dehydroxylation of kaolinite, and formation of meta kaolinite (~ 400–650°C). In the metakaolinite, the Si–O network remains largely intact and the Al–O network reorganizes itself [12,13,17].

4.2. Mineralogical characterization of thermally treated kaolinite samples

The XRD patterns of K1 indicate well crystalline kaolinite mineral. On calcinations, the crystallinity decreased and disordered metakaolinite has been formed at 600°C. During calcinations, aggregate structures may be formed by partial fusion of particles due to the presence of low temperature fusing materials [12,13,17].

4.3. FT-IR spectral analysis

In Fig. 8, the spectrum of K1 indicates characteristic bands of kaolinite mineral at ~3,696, 3,621, 1,100, 1,033, 1,007, 913, 699, 538, 470, and 429 cm^{-1}. Bands of large intensity at region (3,690–3,620 cm^{-1}) represent well-crystallized kaolinite [12,13]. Weak bands in the spectrum of K3 indicate less ordered sample due to thermal treatment.

In the spectrum of malathion-loaded K3, a high intensity broadband covered the region 1,062~1,219 cm^{-1} that indicates a high concentration of Si−O and P−O−C moieties. Weak bands at 1,458, 1,702, 2,341, 2,369 and 2,929 cm^{-1} correspond to $-CH_2$, −C=O, −S−H and −C−H (stretch), respectively. Weak broadbands at 3,449 and 3,576 cm^{-1} may be an indication on the hydroxyl groups of H-bonded water bridge. Minor bands at the region 3,623–3,695 cm^{-1} are for free –OH. Characteristic bands in the region 1,375–1,465 cm^{-1} related to $–CH_3$ and $–CH_2$ groups of malathion spectrum were almost absent in the spectrum of malathion-loaded K3.

5. Desorption studies

The adsorption capacity values of malathion by the studied adsorbents after their regeneration by thermal treatment at 500°C are listed in Table 4. The removal efficiency of adsorbents (except B2) started to decrease after the 3rd run.

The temperature 500°C was an optimum one for the regeneration of the studied adsorbents as indicated by Fig. 9. This is due to the adsorbed malathion completely decomposes before 500°C as indicated by the TGA analysis of malathion-loaded K3.

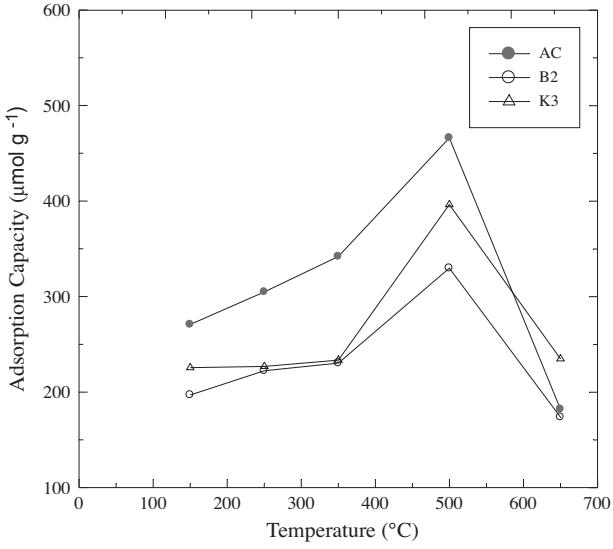

Fig. 9. Regeneration of loaded AC, B2, and K3 as a function of temperature.

6. Conclusion

Effect of calcinations of kaolinite clay mineral on its capacity and efficiency in the removal of malathion from aqueous solution was studied at its natural pH. AC and bentonite were included for comparison. The results obtained indicated that the thermal treatment is a promising method for improving the surface hydrophobicity of the clay mineral without any organic treatment. The calcined kaolinite samples showed greater capacity (q_{max}), faster rate (k_{ads}), and higher affinity towards the hydrophobic adsorbate (malathion) over bentonite samples. So, thermally treated kaolinite can be used as an effective adsorbent for the removal of some organic pollutants such as pesticides and petrochemicals without need for any organic modification when they are similar to malathion in its adsorption behavior.

References

[1] G. Ma, L. Xu, S. Wang, R. Zheng, S. Jin, S. Huang, Y. Huang, Toxicity of 40 herbicides to the green alga Chlorella Vulgaris, Ecotoxicolgy and Environmental Safety, Environ. Res., Sec. B 51 (2002) 128–132.

[2] R.C. Martínez, E.R. Gonzalo, M.E.F. Laespada, F.H. Sánchez San Román, Evaluation of surface- and ground-water pollution due to herbicides in agricultural areas of Zamora and Salamanca (Spain), J. Chromatogr. A 86 (2000) 971.

[3] K. Ohno, T. Minami, Y. Matsui, Y. Magara, Effects of chlorine on organophosphorous pesticides adsorbed on activated carbon: Desorption and oxon formation, Water Res. 42(6–7) (2008) 1753–1759.

[4] M.T. Sng, F.K. Lee, H.Å. Lakso, Solid-phase microextraction of organophosphorous pesticides from water, J. Chromatogr. A 759 (1997) 225–230.

[5] V.K. Gupta, C.K. Jain, I. Ali, S. Chandra, S. Agarwal, Removal of lindane and malathion from wastewater using bagasse fly ash—a sugar industry waste, Water Res. 36 (2002) 2483–2490.

[6] A.L. Gimsing, J.C. Sørensen, B.W. Strobel, H.C.B. Hansen, Adsorption of glucosinolates to metal oxides, clay minerals, and humic acid, Appl. Clay Sci. 35 (2007) 212–217.

[7] J.B. Alam, A.K. Dikshite, M. Bandyopadhayay, Evaluation of thermodynamic properties of sorption of 2,4-D and atrazine by tire rubber granules, Sep. Purif. Technol. 42 (2005) 85–90.

[8] O.R. Pal, A.K. Vanjara, Removal of malathion and butachlor from aqueous solution by clays and organoclays, Sep. Purif. Technol. 24 (2001) 167–172.

[9] B. Witthuhn, T. Pernyeszi, P. Klauth, H. Vereecken, E. Klumpp, Sorption study of 2,4-dichlorophenol on organoclays constructed for soil bioremediation, Colloi. Surf. A: Physicochem. Eng. Aspects 265 (2005) 81–87.

[10] M.J. Sanchez-Martin, M.S. Rodriguez-Cruz, M.S. Andrades, M. Sanchez-Camazano, Efficiency of different clay minerals modified with a cationic surfactant in the adsorption of pesticides: Influence of clay type and pesticide hydrophobicity, Appl. Clay Sci. 31 (2006) 216–228.

[11] E. Bojemueller, A. Nennernann, G. Lagaly, Enhanced pesticide adsorption by thermally modified bentonites, Appl. Clay Sci. 18 (2001) 277–294.

[12] S. Chandrasekhar, S. Ramaswamy, Influence of mineral impurities of kaolin and its thermally treated products, Appl. Clay Sci. 21 (2002) 133–142.

[13] G. Kakali, T. Perraki, S. Tsivilis, E. Badogiannis, Thermal treatment of kaolin: the effect of mineralogy on the pozzolanic activity, Appl. Clay Sci. 20 (2001) 73–80.

[14] C.S. Piper, Soil and Plant Analysis, Interscience Publ., New York, NY, 1950.

[15] M.L. Jackson, Soil Chemical Analysis, Prentice Hall India, New Delhi, 1973.

[16] D. Xu, Z. Xu, S. Zhu, Y. Cao, Y. Wang, X. Du, Q. Gu, F. Li, Adsorption behavior of herbicide butachlor on typical soils in china and humic acids from the soil samples, J. Colloid Interf. Sci. 285 (2005) 27–32.

[17] A.A. Atia, A.M. Donia, R.A. Hussien, R.T. Rashad, Efficient adsorption of malathion from different media using thermally treated kaolinite, Desalin. Water Treat. 30 (2011) 178–185.

[18] F. Gao, Clay/polymer composites: The story, Mater. Today Nov. (2004) 50–55.

[19] P. Rene, Y. Bruno, Use of Modified Clays for Controlling Soil Environmental Quality, Lippincott Williams & Wilkins, Inc. [Context Link]. Ovid Technol., Inc. 166(12) (2001) 880–895.

[20] C.H. Giles, T.H. Macewan, S.N. Nakhwa, D. Smith, Studies in adsorption. Part XI. A system of classification of solution adsorption isotherms, and its use in diagnosis of adsorption mechanisms and in measurement of specific surface areas of solids, J. Chem. Soc. (1960) 3973–3993.

[21] A. Nennemann, S. Kulbach, G. Lagaly, Entrapping pesticides by coagulating smectites, Appl. Clay Sci. 18 (2001) 285–298.

[22] G. Lagaly, Pesticide clay interactions and formulations: Introduction, Appl. Clay Sci. 18 (2001) 205–209.

[23] M.C. Hernández-Soriano, M.D. Mingorance, A. Peña, Interaction of pesticides with a surfactant-modified soil interface: Effect of soil properties, Colloids Surf. A: Physicochem. Eng. Aspects 306 (2007) 49–55.

[24] P.K. Malik, Dye removal from waste water using activated carbon developed from sawdust: Adsorption equilibrium and kinetics, J. Hazar. Mater. 113(1–3) (2004) 81–88.

[25] E. Guibal, C. Milot, J.M. Tobin, Metal-anion sorption by chitosan beads: Equilibrium and kinetic studies, Ind. Eng. Chem. Res. 37 (1998) 1454–1463.

[26] F.D. Aristov, M.M. Tokarev, A. Freni, I.S. Glaznev, G. Restucci, Kinetics of water adsorption on silica, Micropor. Mesopor. Mater. 96 (2006) 65–71.

[27] Y.I. Aristov, I.S. Glaznev, A. Freni, G. Restucci, Kinetics of water sorption on SWS-1L (calcium chloride confined to meso-porous silica gel): Influence of grain size and temperature, Chem. Eng. Sci. 61 (2006) 1453–1458.